Dielectric Properties of Nanostructured ZnO Using Impedance Spectroscopy

Grant Mayberry[a)] and Parameswar Hari[b)]

Department of Physics and Engineering Physics, University of Tulsa, Tulsa, Oklahoma 74104, USA

[a)] *Corresponding author: gmm2929@utulsa.edu*
[b)]*parameswar-harikumar@utulsa.edu*

Abstract. This study focuses on the dielectric properties of 21.9-nm spherical zinc oxide (ZnO) nanoparticles (NPs) at room temperature, as a dry powder and suspended in a liquid. Impedance spectra in the frequency range of 100 Hz to 5.1 MHz were used to investigate the frequency-dependent dielectric properties of ZnO NPs. The commercially available ZnO NPs used in this study were suspended in variable volume fractions up to ~1% in deionized (DI) water and unrefined organic coconut oil and subjected to three sonication conditions: no sonication (NS), 1 hour of bath sonication (BS), and 1 hour of bath sonication followed by probe sonication throughout the experiment (CS, "concurrent sonication") to determine sonication dependence. Small volumes of the resulting suspension were injected sequentially into a dielectric cell for measuring frequency response. Dry particle tests were conducted similarly. Impedance data suggests that the dielectric behavior of ZnO NPs in a liquid suspension is highly dependent on sonication before and during the test and exhibited a strong dependence of dipole with the polarity of the liquid at low frequencies. In addition, a higher dielectric constant of ZnO NPs was observed when the nanoparticles were in suspension than as a dry powder. For frequencies between 100 Hz and 100 kHz, the average dielectric constant of ZnO NPs in DI water, in unrefined coconut oil, and as a dry particle are 368.63, 24.43, and 7.25, respectively.

INTRODUCTION

Nanostructured ZnO has been investigated as an n-type semiconductor material for third-generation photovoltaics. Nanostructured materials have properties that vary wildly and chaotically with size and morphology, often varying greatly from their bulk counterparts [1]. The properties of bulk materials are independent of size. However, there exists some lower limit of this independence. After this point, entirely new properties can be observed from existing materials structured in new ways. Photovoltaics with nanostructured semiconductor materials such as ZnO NPs are much cheaper and cleaner in their construction than silicon-based photovoltaics, but they do not yet offer the high efficiency of silicon-based photovoltaics [2]. Understanding the dielectric and optical properties of nanomaterials is very important in order to improve their efficiency in photovoltaics. Furthermore, the dielectric properties of any material are important for understanding its behavior in solid-state devices and junctions. Although the experiments outlined in this study cover frequencies well below meaningful optical frequencies, the methodology could be extended to higher frequencies to determine the frequency-dependent complex index of refraction for various nonmagnetic nanomaterials. In this study the dielectric constant of suspended particles is determined by the following relation, derived from Ref. [3] (see Appendix A for full derivation):

$$\varepsilon_s^* = \varepsilon_e^*(\varepsilon_r^* - 1)\phi + \varepsilon_e^* \tag{1}$$

where ε_s^* is the complex dielectric constant of a suspension of spherical NPs, ε_e^* is the complex dielectric constant of the suspension media, ϕ is the volume fraction of NPs in suspension, and ε_r^* is the complex dielectric constant of the NPs.

APPARATUS AND METHODOLOGY

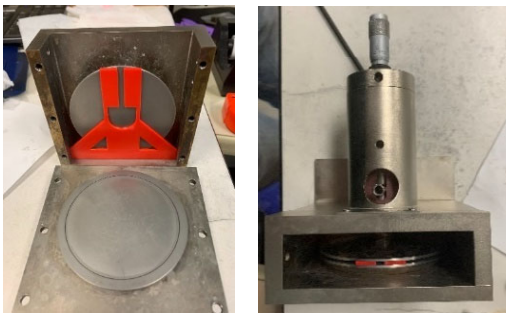

(a) (b)

FIGURE 1. The apparatus used in this study is shown (a) open to reveal the custom 3D-printed model and (b) ready for use. This dielectric cell was constructed from a 2-mm-wide custom 3D-printed PLA (polylactic acid) model, sanded flat, and placed in an IET Labs LD-3 rigid dielectric cell. Kelvin probes were attached to both leads, leading to a Zurich Instruments MFIA impedance analyzer. Liquid samples were injected and solid samples funneled through the long neck at the top of the 3D model. The 3D model was printed with 100% infill and exhibited no permanent deformation throughout the study.

The apparatus shown in Fig. 1 is the product of an iterative process we used to find the ideal equipment to determine the dielectric properties of a small volume of powder. Samples are prepared by measuring out a few tenths of a gram of ZnO NPs into 3 mL of liquid. The resulting suspension is sonicated for an hour to produce a homogenous stock. This is diluted over various amounts into more suspension media and allowed to settle before being subjected to various sonication conditions, and the dielectric constant of each is determined. This is done to produce a curve of dielectric constant vs volume fraction of NPs for each frequency, sonication condition, and suspension media. Each test consisted of injecting 25 μL of test suspension (or ~0.02–0.05 g of powder) and taking impedance spectra from 100 Hz to 5.1 MHz with a test voltage of 300 mV. Ten injections are performed in each test, totaling 250 μL of test suspension in the dielectric cell (or around 0.1 g of powder). By the methods outlined in Ref. [4] and Appendix B, ε_r^* can be determined across all frequencies for any suspended or dry powder from these spectra. This methodology was conducted four times each for ZnO NPs in DI water and three times in coconut oil after no sonication (NS), 1 hour of bath sonication (BS), and 1 hour of bath sonication followed by probe sonication throughout the experiment (CS, "concurrent sonication"), totaling 21 experiments and 210 spectra. In addition, 9 CS coconut oil suspensions were tested (90 spectra), and 14 volumes of powder were tested (14 spectra).

RESULTS

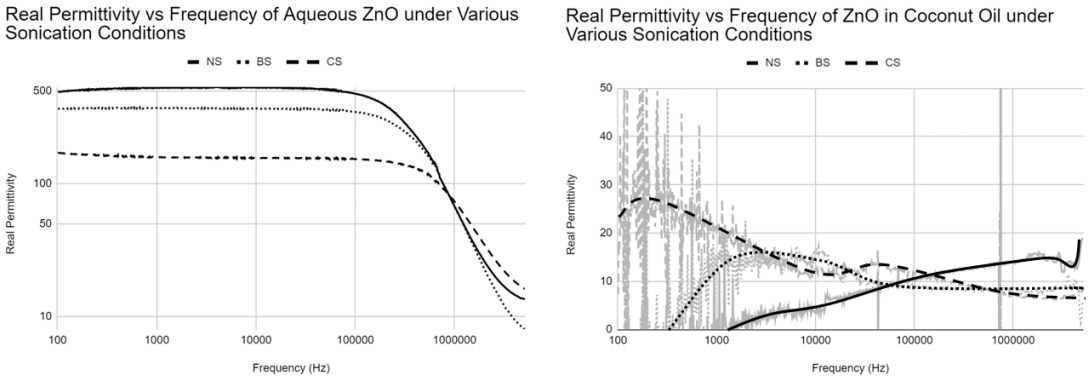

(a) (b)

FIGURE 2. The sonication dependence of the real component of the dielectric spectra of ZnO NPs in (a) DI water and (b) coconut oil. The noisy appearance of the dielectric spectra in coconut oil can be attributed to the high resistivity of coconut oil. The solid dotted and dashed lines represent the dielectric constants for ZnO NP suspensions subjected to NS, BS, and CS, respectively.

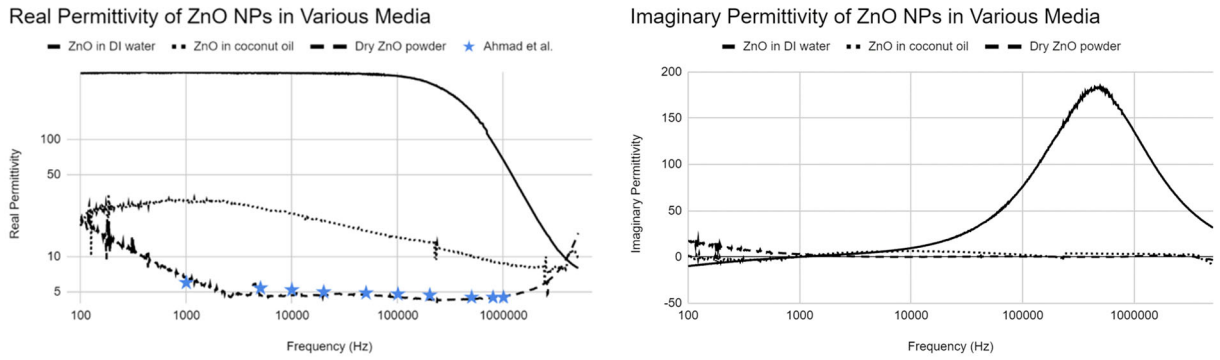

(a) (b)

FIGURE 3. The (a) real and (b) imaginary components of the dielectric constant of ZnO NPs suspended in each fluid. The solid, dotted, and dashed lines represent the dielectric properties for ZnO NPs in water subjected to BS, coconut oil subjected to CS, and dry air, respectively. Note that Figs. 2 and 3 do not match up concerning coconut oil. This is because of the additional 9 CS coconut oil experiments included in Fig. 3. Data from previous literature is highlighted as well [5].

The experiments in sonication dependence shown in Fig. 2 show that CS yielded the most repeatable results in coconut oil ($R^2 \approx 1$ for Eq. (1) for most frequencies). This is not the same for DI water, possibly due to the physically invasive probe sonicator and the solvent and conductive nature of DI water. In any case, BS provided the most reliable results ($R^2 \approx 1$ for Eq. (1) for most frequencies) in DI water. As shown in Fig. 2, regardless of sonication condition, ZnO NPs exhibit a higher dielectric constant across the spectrum in DI water (δ≈2.95 [6]) than in coconut oil (δ very low, nonpolar). This is consistent with Fig. 3. Although 14 dry powder tests were conducted, only 7 were included in Fig. 3, due to the NPs exhibiting charging behavior. When the charged and uncharged data were separated, it was clear the charged particles exhibited a much higher dielectric constant. This data was not included in Fig. 3 to maintain consistency. This charging may also explain the sudden increase in dielectric constant at higher frequencies in dry ZnO NPs; such an increase was not observed in the charged powder dielectric spectra.

CONCLUSIONS

Figure 2 demonstrates the claim that the dielectric properties of suspended ZnO NPs are highly dependent on sonication, showing the importance of material distribution in dielectrics made of multiple materials. The CS experiments in coconut oil and BS experiments in DI water hold the most meaningful data as large complexes of coalesced particles are continually redistributed, meaning the assumptions made in Eq. (1) are valid. Figure 3 demonstrates that ZnO NPs are a stronger dipole in more polar fluids at low frequencies. The ZnO NPs exhibit a real dielectric component at ~370 when suspended in DI water at low frequencies, while only reaching ~30.7 over the same range when suspended in coconut oil. As a dry powder, ZnO NPs exhibit dielectric constants in the single digits ($\varepsilon \approx 4$–7, from 1 kHz to 1 MHz, consistent with previous literature [5]). Across the majority of test frequencies, suspended ZnO NPs exhibited higher dielectric constants than dry powder, shown in Fig. 3.

ACKNOWLEDGMENTS

We would like to thank the University of Tulsa Department of Physics and Engineering Physics for their facilities, Ganga Neupane for his expertise in the operation of Zurich Instruments, Richard Portman and Rusiri Rathnasekara for their assistance preparing and imaging TEM images, Gabriel LeBlanc for the use of his lab equipment and 3D printing expertise, and the Oklahoma Photovoltaic Research Institute.

REFERENCES

1. G. Guisbiers, S. Mejía-Rosales, and F. Deepak, J. Nanomater., **2012**, 1 (2012).
2. A. Wibowo, M. Marsudi, M. Amal, M. Ananda, R. Stephanie, H. Ardy, and L. Diguna, RSC Adv. **10**, 42838 (2020).

3. C. Grosse and V. Shilov, J. Colloid Interface Sci. **309**, 283 (2007).
4. A. Kordzadeh and N. de Zanche, Concepts Magn. Reson. **46**, 19 (2016).
5. P. Ahmad, A. Rao, K. Babu, and G. Rao, Mater. Chem. Phys. **224**, 79 (2019).
6. A. Gubskaya and P. Kusalik, J. Chem. Phys. **117**, 5290 (2002).

Supporting materials are available online at https://www.spsnational.org/jurp.

APPENDIX A – DERIVATION OF EQ. (1)

Suppose

$$\varepsilon_s^* = \varepsilon_e^*(1 + 3d^*\phi) \quad [3] \tag{A.1}$$

where ε_s^* is the complex dielectric constant of a suspension of spherical NPs, ε_e^* is the complex dielectric constant of the suspension media, d^* is the complex dipole coefficient of the NPs, and ϕ is the volume fraction of NPs in suspension, and

$$\frac{<p^*>}{4\pi\varepsilon_0} = d^* a^3 E^* \quad [3] \tag{A.2}$$

where $< p^* >$ is the average complex dipole moment of each NP, ε_0 is the permittivity in free space, E^* is the complex electric field in the suspension, and a is the radius of the NPs, which becomes

$$P^* = 3\varepsilon_0 d^* E^* \tag{A.3}$$

where P^* is the average polarization of each NP. Thus

$$D^* = E^*\varepsilon_0 + 3\varepsilon_0 d^* E^* \tag{A.4}$$

where D^* is the complex electric displacement in the suspension, and

$$D^* = \varepsilon_0 E^*(1 + 3d^*) \tag{A.5}$$

meaning

$$\varepsilon_r^* = 1 + 3d^* \tag{A.6}$$

where ε_r^* is the complex dielectric constant of the NPs. Combining with Eq. (A.1), this yields Eq. (1):

$$\varepsilon_s^* = \varepsilon_e^*(\varepsilon_r^* - 1)\phi + \varepsilon_e^* \tag{A.7}$$

APPENDIX B – ANALYSIS SPECIFICS

Each individual impedance spectrum was analyzed between 1 and 5.1 MHz and modeled to the equivalent circuit shown in Fig. B-1 by the following representative equation in Zfit [4]:

$$Z = R_s + j\omega L_s + \frac{1}{\frac{1}{R_d} + j\omega(C_0 + C_d)} \tag{B.1}$$

where

$$C = C_0 + C_d = C_0 + mV \tag{B.2}$$

where V is the total injected volume of test suspension/powder and m is the volumetric capacitance of the injected suspension.

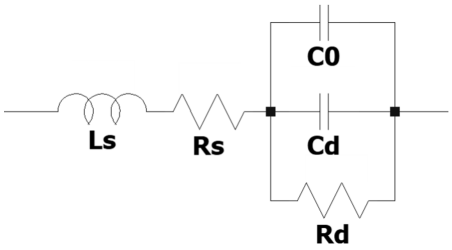

FIGURE B-1. Equivalent circuit used in Zfit to determine the frequency response of the dielectric cell, designed to model a transmission line.

Note that in Eq. (B.1), R_s and L_s are calculated as constant from 1 to 5.1 MHz and assumed to be constant across all frequencies. C and Rd are calculated at every individual frequency. The resulting m value shown in Eq. (B.3) correlates directly to the dielectric constant of the suspension by

$$\varepsilon_s = \frac{m}{m_0}(\varepsilon_w - 1.0006) + 1.0006 \tag{B.3}$$

where m_0 is the volumetric capacitive dependence of DI water between 1 and 5.1MHz (determined experimentally), and ε_w is the dielectric constant of DI water over that frequency range (~80.42). The determination of dielectric loss is more complex:

$$\frac{1}{R_d} = \sigma = \sigma_0 + \varepsilon_v'' V\omega K \tag{B.4}$$

where σ is the parallel conductance of the system, σ_0 is the conductance of the system with no injected volume, ε_v'' is the volumetric dielectric loss of the suspension, V is the injected volume, and K is given by

$$K = 0.00314785 m_0 = m_0 \frac{0.25}{80.42 - 1.0006} \tag{B.5}$$

Equation (B.4) can be solved by linear regression, where injected volume is the independent variable, to determine σ_0. Thus

$$\varepsilon_s'' = \frac{\sigma - \sigma_0}{\omega K} \cdot \frac{V_{max}}{V} \tag{B.6}$$

where $V_{max} = 0.25$ mL, the largest test volume, and ε_s'' is the dielectric loss of the suspension, averaged across all volumes. Thus the complex dielectric constant of the suspension is given by

$$\varepsilon_s^* = \varepsilon_s - j\varepsilon_s'' \tag{B.7}$$

APPENDIX C – TRANSMISSION ELECTRON MICROSCOPY (TEM) CHARACTERIZATION

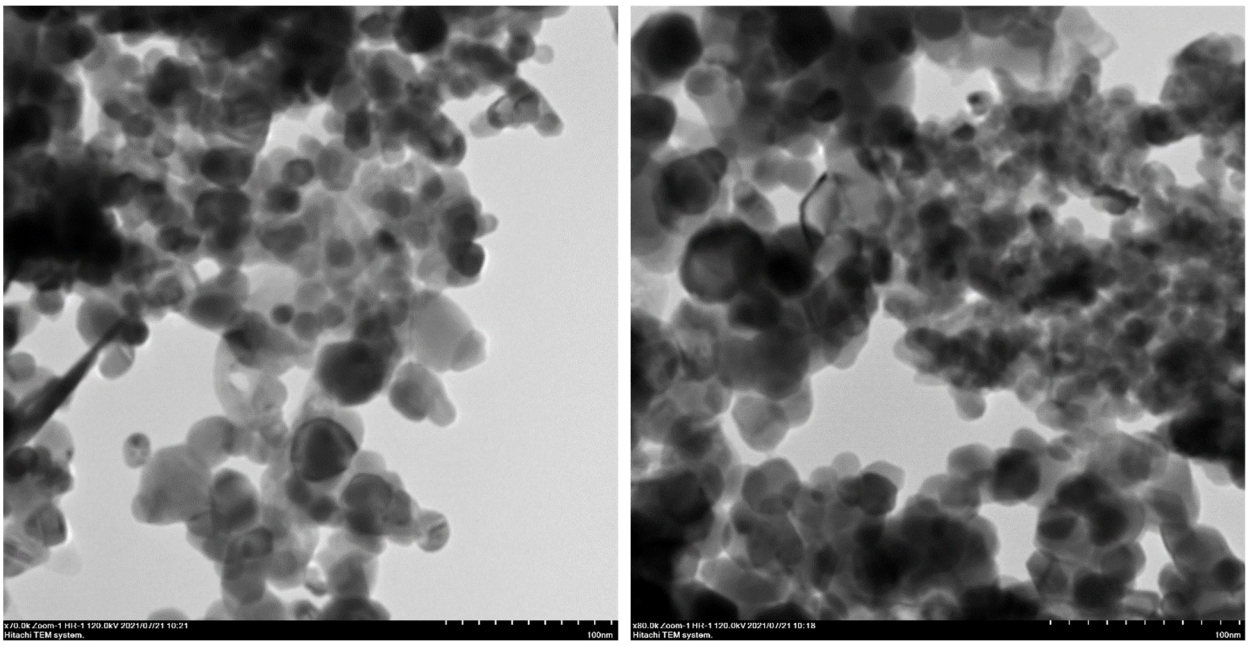

FIGURE C-1. TEM images, provided by Richard Portman, of the ZnO NPs used in this study. As seen here, most of the particles are uniform (~21.9 nm in diameter) and spherical, with a few larger outliers. (Note the 100-nm scale at the base of each image.) These are the result of a small volume (~10 μL) of NPs suspended in toluene and sonicated for 15 minutes.

TEM images of the NPs used in this study are seen in Fig. C-1. The 18 hours between sonication and imaging is believed to have contributed to the clumping of particles into large groups, leaving much of the imaging surface blank. This motivated the study of the dependence of the dielectric properties on sonication.